Carbon density in boreal forests responds non-linearly to temperature: An example from the Greater Khingan Mountains, northeast China

Yang Liu, Ralph Trancoso, Qin Ma, Philippe Ciais, Lidiane P Gouvêa, Chaofang Yue, Jorge Assis, Juan A Blanco

Agricultural and Forest Meteorology 338 (2023) 109519

Contents lists available at ScienceDirect

Agricultural and Forest Meteorology

journal homepage: www.elsevier.com/locate/agrformet

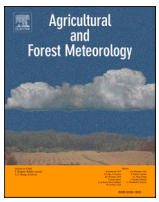

Carbon density in boreal forests responds non-linearly to temperature: An example from the Greater Khingan Mountains, northeast China

Yang Liu [a], Ralph Trancoso [b], Qin Ma [c], Philippe Ciais [d], Lidiane P. Gouvêa [e], Chaofang Yue [f], Jorge Assis [e,g], Juan A. Blanco [h,*]

[a] College of Forestry, Inner Mongolia Agricultural University, Hohhot 010019, China
[b] School of Biological Sciences, University of Queensland, Brisbane, Queensland 4072, Australia
[c] School of Geography, Nanjing Normal University, Nanjing 210023, China
[d] Laboratoire des Sciences du Climat et de l'Environnement, LSCE/IPSL, CEA-CNRS-UVSQ, Université Paris-Saclay, Gif-sur-Yvette 91191, France
[e] CCMAR - Centre of Marine Sciences, University of Algarve, Faro, Portugal
[f] Forest Res Inst Baden Wurttemberg, Wonnhaldestr 4, Freiburg D-79100, Germany
[g] Faculty of Bioscience and Aquaculture, University of Nord, Bodø, Norway
[h] Departamento de Ciencias, Institute for Multidisciplinary Research in Applied Biology, Universidad Pública de Navarra, Campus de Arrosadía, Pamplona, Navarra 31006, Spain

ARTICLE INFO

Keywords:
Boosted regression trees
Carbon storage
Carbon storage change
Climate influences
Forest vegetation
Temperature threshold

ABSTRACT

Boreal forests play a crucial role in the global carbon (C) cycle and in climate stabilization. To better predict global C budgets, it is important to accurately estimate the size of forest C pools, and to identify the factors affecting them. We used national forest inventory data for the Greater Khingan Mountains, northeast China from 1999 to 2018 and 149 additional field plots to estimate C storage and its changes in forest vegetation, excluding C stored in soils, and to calculate the total C density in forest ecosystems. From 1999 to 2018, the vegetation C storage and density increased by 92.22 Tg and 4.30 Mg C ha^{-1}, respectively, while the mean C sink was 4.61 Tg C yr^{-1}. Carbon storage and density showed the same pattern, with the largest stocks in trees, followed by herbs, shrubs, and then litter. Mean C density was higher in mature forests than in young forests. The maximum C density was recorded in *Populus davidiana* forests, and was 2.2-times larger than in *Betula davurica* forests (the minimum). The mean (± standard error) total C density of forest ecosystems was 111.3 ± 2.9 Mg C ha^{-1}, including C stored in soils. Mean annual temperature (MAT) controlled total C density, as MAT had positive effects when it was lower than the temperature of the inflection point (-2.1 to -4.6 °C) and negative effects when it was above the inflection point. The rate of change in the total C density depended on the quantile points of the conditional distribution of total C density. Natural and anthropogenic disturbances had weaker effects on C density than temperature and precipitation. In conclusion, our results indicate that there might be a temperature-induced pervasive decrease in C storage and an increase in tree mortality across Eastern Asian boreal forests with future climate warming.

1. Introduction

Forests cover 31% of the global land area (FAO, 2020), storing approximately 45% of the total terrestrial carbon (C) (Silva and Anand, 2013). The current C stock in the world's forests is estimated to be 861 Pg C (Pan et al., 2011), while in China's forest ecosystems is 79.24 Pg (Tang et al., 2018). Boreal forests account for approximately 30% of the total C stored in forest ecosystems (Dixon et al., 1994), and play a major role in the global C cycle (Ma et al., 2012). Forests are also a safe haven for biological communities threatened by climate change (Kauppi and Posch, 1985). However, C storage and ecosystem services in boreal forests are threatened by increasingly altered disturbance regimes (Bradshaw et al., 2009).

The forests on the Greater Khingan Mountains form the southern boundary of the boreal forests in eastern Asia (Li et al., 2020). Predictions under a warmer global climate show that the dominant species, Dahurian larch (*Larix gmelinii* (Rupr.) Rupr.), is likely to retreat northward (Bai et al., 2019), with replacement by species better suited to a

* Corresponding author.
E-mail address: juan.blanco@unavarra.es (J.A. Blanco).

https://doi.org/10.1016/j.agrformet.2023.109519
Received 6 September 2022; Received in revised form 10 May 2023; Accepted 14 May 2023
Available online 23 May 2023

temperate climate (Bu et al., 2008; Kirilenko and Sedjo, 2007). Recent climate change is already affecting the C balance of forests in the Greater Khingan Mountains with more frequent stand-replacing wildfires (Liu et al., 2012), reduced tree growth (Zhang et al., 2018), drought-induced tree mortality (Bai et al., 2019), and changes in forest species' composition (Bonan, 2008).

The Greater Khingan Mountains account for approximately 10% of China's forest area (DFPRC, 2014) and play a critical role in the national C budget. Thus, an accurate estimation of the C dynamics and C density of forest vegetation is vital to assess potential responses to climate change, and to identify changes in the amounts of C released from forests when forest ecosystems are disturbed or changed. Previous studies have explored the spatial and temporal variations in, and distribution patterns of, C storage and density in forest ecosystems at global (e.g., Dixon et al. (1994), Pan et al. (2011), Guo et al. (2019)), national (e.g., Cannell and Milne (1995), Tang et al. (2018)), regional (e.g., Holland and Brown (1999), Chen et al. (2019)) and forest-stand scales (e.g., Ray et al. (2011), Liu et al. (2014a)). However, there are no accurate estimates of C storage and density in forest ecosystems in the boreal forests of the Greater Khingan Mountains because of accessibility constraints, a typical situation for the boreal forests of Northeast Asia.

Forest ecosystems are affected by many biotic and abiotic factors such as forest type, stand age, disturbances, climate, soil factors, and elevation (Houghton, 2001; Zhu et al., 2010). There is also a strong relationship between C stocks and biodiversity in terrestrial ecosystems (Strassburg et al., 2010). Biodiversity can make ecosystems more resilient and more productive (Flombaum and Sala, 2008), which increases C sequestration. For example, Zhou et al. (2008) reported higher C densities in mixed coniferous and broadleaved forests than in pure forests of each kind.

Disturbance dynamics are particularly important in boreal zones. They are mainly driven by natural processes such as fire, followed by insect outbreaks, and to a lesser extent by human activities (mainly deforestation or logging) because human populations are relatively sparse (Soja et al., 2007). Disturbances that alter forest nutrient reserves can ultimately lead to the emission of vast amounts of C into the atmosphere (Bhatti et al., 2002). Disturbances are also directly linked to stand age in boreal forests as they are the main causes of stand replacement. Forest C storage generally increases with stand age (Houghton, 2001; Pregitzer and Euskirchen, 2004). In boreal forests, however, C storage tends to increase with stand age for the first 120 years, but then decrease when the stands are more than 200 years old (Pregitzer and Euskirchen, 2004). Chen et al. (2016) also found that stand age was an important factor controlling C storage in boreal forests. These studies suggest that it is essential to differentiate age classes to get an accurate estimate of C storage in boreal forests.

In addition, C storage in forest ecosystems is driven by interactions among climate, soil factors such as moisture, temperature, nutrients and soil texture, and disturbance regimes (Li et al., 2022a). These factors control primary production and decomposition, which in turn affect C dynamics (Bhatti et al., 2002; Bonan and Cleve, 1992). The forest type, biodiversity, climate variables, and soil factors all change with elevation, and C storage in forest ecosystems also varies substantially along an altitudinal gradient (Zhu et al., 2010). Climate change is a major driver of variations in forest C dynamics (Shugart et al., 2003). Some studies report a positive association—the enhanced atmospheric CO_2 concentrations, increased warmth, and extended growth seasons promote tree growth and increase C storage (Kirilenko and Sedjo, 2007; Sohngen and Sedjo, 2005). However, other studies report a negative association because the combination of climate warming and drought tends to decrease tree growth and increase tree mortality, which undermines C storage (Liu et al., 2013; Ma et al., 2012; Michaelian et al., 2011). Previous studies on Northeastern Asian boreal forests have rarely studied the relative contribution of multiple factors to current C dynamics. Therefore, the mechanisms influencing the amount and rate of C storage in the Greater Khingan Mountains and their surrounding boreal region remain unclear.

Given the research gaps mentioned above, we formulated the following hypotheses for Eastern Asia's boreal forests: (1) forest age and species composition are main structural drivers of C density; and (2) climate drivers affect C density, but their relationships with C density are not linear. When testing these hypotheses, our aims were as follows: (1) to estimate the amount of C stored in forest vegetation of the whole Greater Khingan Mountains from 1999 to 2018; (2) to explore whether and how climate, soil, biodiversity, elevation, stand age, forest type, and disturbances affect the C density in forest ecosystems; and (3) to establish a quantitative relationship between the dominant driver and total C density in forest ecosystems.

2. Methods

2.1. Study area

The Greater Khingan Mountains (46°26′–53°34′ N, 119°30′–127°10′ E), with a total area of 24.7 × 10^4 km^2, are situated in northeast China and extend across the Inner Mongolia Autonomous Region and Heilongjiang Province in the cold temperate zone (Fig. 1). The forests in the Greater Khingan Mountains form the southern boundary of eastern Asia boreal forests and are dominated by L. *gmelinii* (Editorial Committee for Vegetation of China, 1980). Other conifer species include Scots pine (*Pinus sylvestris* L. var. *mongolica* Litv.), Korean spruce (*Picea koriensis* Nakai), and Yezo spruce (*Picea jezoensis* (Lindl.) Carrière var. *microsperma* (Lindl.) Cheng et Fu). The main broad-leaved tree species include white birch (*Betula platyphylla* Suk.), aspen (*Populus davidiana* Dole), and Mongolian oak (*Quercus mongolica* Fisch. ex Ledeb.) (Xu, 1998). The understory and ground vegetation composition vary with edaphic and topographic conditions (Wang et al., 2001). The average annual temperature is approximately -3 °C. The average monthly maximum and minimum temperatures are 18.2 °C in July and -27.5 °C in January, respectively. The annual total precipitation (rainfall plus snowfall water equivalent) ranges between 300 and 500 mm, the majority of which is concentrated in the period from May to October. The elevation of the Greater Khingan Mountains ranges from 330 to 1750 m a.s.l. (Imbert et al., 2021; Xu, 1998). Slopes are moderate, with more than 80% being gentle slopes (<15°). Snow cover lasts for 5 months and averages 300–500 mm and the frost-free period is shorter than 100 days (Liu et al., 2020a; Xu, 1998). The depth of the permafrost varies from 5 to 40 m, with a maximum of 120 m. The predominant soil type is dark brown forest soil (Haplumbrept or Eutroboralf) (Imbert et al., 2021). Historically, forest resources were abundant in the Greater Khingan Mountains. However, over the past 70 years, forests have been degraded by wildfires, excessive deforestation, and logging (Hu et al., 2018). To reduce degradation, the Natural Forest Protection project was initiated in 1998 and commercial harvesting at the study area has been prohibited since April 1st, 2015.

2.2. Data sources and collection

The first data source used in this study was the national forest inventory of China for the Greater Khingan Mountains for the periods 1999–2003, 2004–2008, 2009–2013, and 2014–2018 (see Supporting Information Appendix 1). These data provided information about plot areas, dominant tree species, age classes (young, half-mature, near mature, mature, and over mature), and the diameter at breast height (DBH, 1.3 m above the ground), total tree height (*H*), and tree species for all trees with DBH > 5 cm. National forest inventory field plots were classified into forest types depending on the dominant species (see Supporting Information Appendix 1 for definitions of dominant species). The classification criteria for the five different age classes of the dominant tree species in the plots followed the standard methodology applied in Chinese forest inventories (Supporting Information Table S1) (SFAPRC, 2011). Individual tree volumes for each plot were estimated

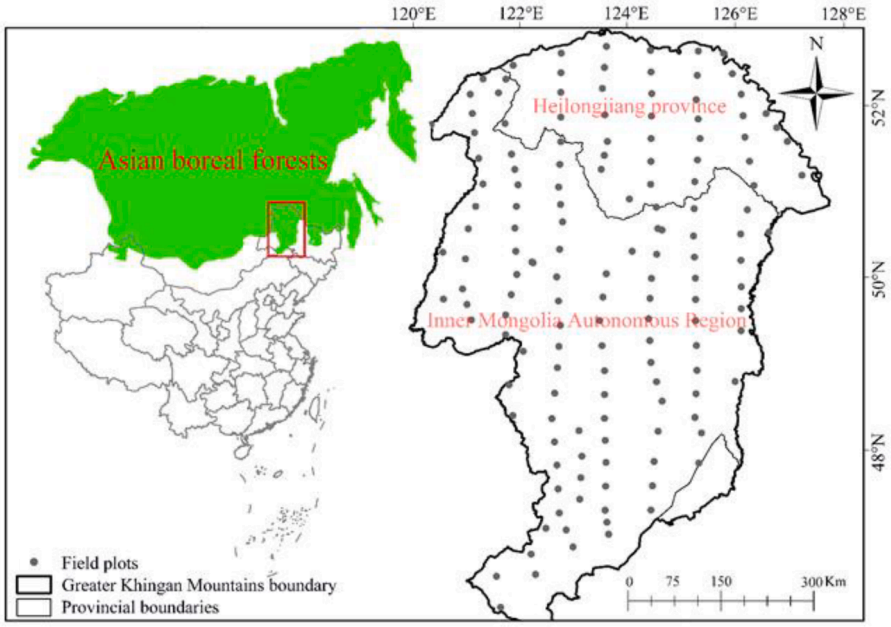

Fig. 1. Location of the Greater Khingan Mountains and 149 field sites sampled from 2015 to 2018 across this area.

using the general volume table (Supporting Information Table S2) (Liu et al., 2017), then summed, and then the result was divided by the plot area to give stand volume (m^3 ha^{-1}). The forest area and stand volume for each age class of different forest types were recorded at the field sample plots from national forest inventories.

The second dataset was from 149 field plots (Fig. 1) with areas ranging from 0.1 to 1.05 ha. These plots were sampled from 2015 to 2018 using a systematic random sampling method, and were distributed across the Greater Khingan Mountains (a minimum of 132 field plots was determined to be required for statistical representativeness to estimate the C density of forest ecosystems and forest vegetation, and to examine the potential drivers of forest ecosystem C density changes in the Greater Khingan Mountains; see Supporting Information Appendix 2 for a detailed determination of the minimum sample size). Similar data to those obtained in the national forest inventory were collected at each plot, including the area, latitude and longitude, and stand age, DBH, *H*, and tree species for all trees with DBH > 5 cm. The methods used to categorize forest type and age class, and to estimate stand volume in 149 field plots were the same as those used in the national forest inventories.

Following a chronosequence approach, we used the 149 field plots to estimate the amount of C stored in the shrub, herb, and litter layers during the periods of 1999–2003, 2004–2008, 2009–2013, and 2014–2018, because the national forest inventory data did not provide information for these layers. The aboveground and belowground biomass were measured in three quadrats along the diagonal of each field plot for shrubs, herbs, and litter using the harvest method (see Section 2.4 for details). Additionally, the names and frequency of the species present in each quadrat were recorded to characterize species diversity in the forest community. The data for the 149 field plots were also used to calculate the C density of forest ecosystems and the C density of forest vegetation. Then, the calculated C density of forest vegetation was compared with that estimated using the national forest inventory data from 1999 to 2018.

2.3. Estimation of C storage in trees among forest types and age groups

Carbon storage in trees varies with forest type and age group Pan et al., 2004). We estimated C based on a volume-to-biomass method that is widely used for estimating C storage in trees including stems, branches, leaves, and roots, i.e., aboveground and belowground biomass C, as given by Eqs. (1) and ((2) (Chen et al., 2019; Fang et al., 2001):

$$CS_{tree_i} = \sum_{j=1}^{m} (a + bV_{ij}) \cdot A_{ij} \times 0.5 \quad (1)$$

$$CS_{tree} = \sum_{i=1}^{n} CS_{tree_i} \quad (2)$$

where CS_{tree_i} (Mg) is C storage in trees of the *i*th forest type ($i = 1, 2, \ldots, 9$); V_{ij} (m^3 ha^{-1}) is forest volume in trees of the *j*th age groups ($j = 1, 2, 3, 4, 5$) in the *i*th forest type; A_{ij} (ha) is area of the *j*th age groups in the *i*th forest type; *a* and *b* are parameters that are constants for an age group of a forest type (see Table S3); 0.5 is the C concentration in the tree layer (Fang et al., 2001); and CS_{tree} (Mg) is C storage in trees. We used the conventional IPCC fraction of 0.50 biomass-to-carbon because even though C content varies slightly among different tree components of the same species (Shen et al., 2016) and among forests with different tree species composition, age, and stand structure (Johnson and Sharpe, 1983; Karjalainen, 1996), it has been argued that using 0.50 wood C content will commonly deviate by only ~2%–3%, resulting in a minor systematic bias of approximately 4–6% in C storage estimates (Thomas and Malczewski, 2007). We considered that such a bias is small compared with other uncertainties related to forest C estimates. In addition, accurate C content data are not available for each type of vegetation biomass, and so the IPCC's default value of 0.50 is generally used (Houghton et al., 1990; IPCC, 2006). Carbon density was estimated by Eq. (3):

$$CD_{tree} = \sum_{i=1}^{n} CS_{tree_i} \Big/ \sum_{i=1}^{n} \sum_{j=1}^{m} A_{ij} \quad (3)$$

where CD_{tree} (Mg C ha^{-1}) is C density in trees, and the other variables are as defined above.

2.4. Estimation of C storage in understory and litter layers in different forest types and age groups

A true year-to-year dataset of C density in shrubs, herbs, and litter for different forest types during the 1999–2018 time span could not be obtained. However, to account for the temporal change in C density in

shrubs, herbs, and litter we used a chronosequence approach. We estimated C density in shrubs, herbs, and litter based on age classes representative of forest growth stages for different forest types, similar to the methods of Pan et al. (2004). These estimates are only accurate at the age class level, rather than at the specific year level. Therefore, the C density in shrubs, herbs, and litter of the same forest types and same age classes was hypothesized to be constant. To calculate C storage in the shrub layer (including aboveground and belowground biomass C), shrubs were harvested from three subquadrats (2 × 2 m) along the diagonal of each field plot. The aboveground biomass of shrubs was clipped and roots excavated. Each component was weighed directly to determine fresh weight. Subsamples of fresh samples of each component were randomly collected to determine moisture content by drying at 85 °C to constant weight; and to determine C content by the potassium dichromate ($K_2Cr_2O_7$) oxidation method. The dry biomass of each component was calculated by multiplying the fresh weight by the dry/fresh weight ratio. Aboveground and belowground C storage in the shrub layer were estimated by multiplying the dry mass of each component (i.e., aboveground and belowground dry biomass stored in shrubs) collected from each plot and the C concentration in the corresponding component (aboveground and belowground of the shrub layer), respectively. Total C storage in shrubs was calculated by summing the C stored in aboveground (leaves, branches, and stems) and belowground (roots) parts. Herbs were collected from three subquadrats (1 × 1 m) arranged along the diagonal line of each field plot, and were separated into aboveground and belowground components. Each fraction was analyzed in the laboratory to determine the C concentrations in aboveground [c] and belowground parts [C]. Total herb C storage was calculated as: (aboveground biomass × aboveground [c]) + (root biomass × root [C]). Litter biomass was collected separately for the upper L layer (intact and relatively undecomposed materials) and the lower F and H layers (fragmented or decomposed materials). We calculated the C storage in litter layers using the same method as described for the herb layer. The C storage and C density in the understory (including aboveground and belowground biomass C) and litter layers were estimated using Eqs. (4)–(7):

$$CD_{shrub_{ij}/herb_{ij}/litter_{ij}} = B_{shrub_{ij}/herb_{ij}/litter_{ij}} \times c_{shrub_{ij}/herb_{ij}/litter_{ij}} \quad (4)$$

$$CS_{shrub_i/herb_i/litter_i} = \sum_{j=1}^{m} CD_{shrub_{ij}/herb_{ij}/litter_{ij}} \times A_{ij} \quad (5)$$

$$CS_{shrub/herb/litter} = \sum_{i=1}^{n} CS_{shrub_i/herb_i/litter_i} \quad (6)$$

$$CD_{shrub/herb/litter} = CS_{shrub/herb/litter} \Big/ \sum_{i=1}^{n}\sum_{j=1}^{m} A_{ij} \quad (7)$$

where $CD_{shrub_{ij}}$, $CD_{herb_{ij}}$, and $CD_{litter_{ij}}$ (Mg C ha^{-1}) is the C density of the shrub, herb, and litter layer, respectively, of the *j*th age groups in the *i*th forest type, which are constants for an age group of a forest type (see Supporting Information Appendix 3 for a detailed estimation of C density in the shrub, herb, and litter layers); $B_{shrub_{ij}}$, $B_{herb_{ij}}$, and $B_{litter_{ij}}$ (Mg ha^{-1}) is the biomass density of shrub, herb, and litter layer, respectively, of the *j*th age groups in the *i*th forest type; $c_{shrub_{ij}}$, $c_{herb_{ij}}$, and $c_{litter_{ij}}$ is the C concentration in the shrub, herb, and litter layer, respectively, of the *j*th age groups in the *i*th forest type; CS_{shrub_i}, CS_{herb_i}, and CS_{litter_i} (Mg) is C storage in the shrub, herb, and litter layer, respectively, of the *i*th forest type; A_{ij} (ha) is area of the *j*th age groups in the *i*th forest type; CS_{shrub}, CS_{herb}, and CS_{litter} (Mg) is C storage in the shrub, herb, and litter layers, and CD_{shrub}, CD_{herb}, and CD_{litter} (Mg ha^{-1}) is C density in the shrub, herb, and litter layer, respectively.

Notably, the calculation of C storage in forest vegetation included the aboveground and belowground (root) C storage in trees, shrubs, and herbs and C storage in litter. Finally, total vegetation C storage was estimated using Eq. (8):

$$CS_{veg} = CS_{tree} + CS_{shrub} + CS_{herb} + CS_{litter} \quad (8)$$

where CS_{veg} (Mg) is C storage in forest vegetation, and the other variables are as defined above.

A univariate analysis of variance (ANOVA) was used to test whether C density was statistically different among different components of forest vegetation (tree, shrub, herb, and litter), among age classes, and among forest types. A *p* value of 0.05 or less was defined as statistically significant (i.e., Tukey's HSD, $p < 0.05$).

2.5. Changes in C storage in forest vegetation

Annual increase in C storage illustrates the speed of tree growth in a certain period, and is a measure of the change in the C storage capacity of a stand over time (Liu et al., 2014b). The annual increase in C storage in trees, shrubs, herbs, litter, or vegetation in the Greater Khingan Mountains, northeast China was calculated for each interval period using Eq. (9) (Brown et al., 1988; Liu et al., 2014b):

$$CSI_{annual} = (CS_t - CS_{t-n})/n \quad (9)$$

where CSI_{annual} (Tg C y^{-1}) is the annual increase in C storage in trees, shrubs, herbs, litter, or vegetation between the *t*th year and *t* − *n*th year; CS_t (Tg) is the amount of C stored in trees, shrubs, herbs, litter, or vegetation in inventory *t* at the end of the interval; $CS_{t\text{-}n}$ (Tg) is the amount of C stored in trees, shrubs, herbs, litter, or vegetation in inventory *t*−*n* at the beginning of the interval; and *n* is the number of years between inventories; $n = 5$ years in this study.

2.6. Estimation of C density in soils and total C density

Soil data were taken from the International Soil Reference and Information center (ISRIC) database on world soil properties (WISE30sec), which are estimated at 1 km spatial resolution (Batjes, 2015) and can be accessed through the ISRIC's Soil Data Hub (http://www.isric.org/explore/wise-databases). Before using the gridded soil data from the WISE30sec, a quality test was carried out by comparing the gridded data with data from 48 actual analyses of soils at the same geographic coordinates (Fig. S1 and Table S7). Soil organic C density (SOCD) values were validated using the Wilcoxon rank-sum test, which is a nonparametric two-sample test. We found that there were no significant statistical differences ($p = 0.126$ and correlation coefficient = 0.76) between actual SOCD measurements from 48 field-based soil studies in the Greater Khingan Mountains and gridded SOCD values extracted from the WISE30sec dataset for the same geographical coordinates (see Appendix 4 in the Supplementary Information for details). Hence, we used the gridded data to calculate the surface SOCD in the upper 20-cm soil layer for different forest types and age classes. We selected the upper 20 cm soil layer because it contains most of the biologically active C (Crowther et al., 2016) and in northern forest soils it can store up to 57% of total soil C (Jobbágy and Jackson, 2000). SOCD was calculated using Eq. (10):

$$SOCD = \rho C D(1-\theta) \times 10^{-1} \quad (10)$$

where *SOCD* is the soil organic C density (Mg C ha^{-1}) at 0–20 cm depth, ρ is the bulk density (g cm^{-3}), *C* is the organic C content (g kg^{-1}), *D* is the depth of soil layer (cm) (*D* is equal to 20 cm for this study), and θ is the volume percentage of coarse fragments (>2 mm). The values of soil variables ρ, *C*, and θ above were extracted from the WISE30sec dataset using corresponding geographic coordinates.

Total C density in forest ecosystems was estimated during the monitoring years using Eq. (11):

$$CD_{eco} = CD_{tree} + CD_{shrub} + CD_{herb} + CD_{litter} + SOCD \quad (11)$$

where CD_{eco} (Mg C ha^{-1}) is C density in forest ecosystems, and the other

variables are as defined above.

2.7. Quantitative relationships between total C density and environmental variables using boosted regression trees modeling and quantile regression

Nineteen environmental predictors, both biotic and abiotic, for the C density of the 149 sites were selected according to their ecological importance for boreal forests (for details, see Appendix 5, Supplementary Information Table S8). The predictors included numerical variables of climate, soil, biodiversity, elevation, stand age, forest type, and disturbance. The dummy variable method was used to convert the forest type into a numerical variable (Table S9). Disturbance events were quantified using the remote-sensing derived delta Normalized Burn Ratio method (see Appendix 5).

Before modeling, Pearson's correlation coefficients were calculated for all pairs of predictors to identify multicollinearity among variables. In this step, four pairs of predictors were found to be strongly correlated (Pearson's correlation > 0.9; Fig. S2). Therefore, a principal component analysis (PCA) was applied to each of these pairs to reduce and decompose data dimensions into their first components (e.g., De Marco and Nóbrega (2018)). Ultimately, 16 variables were available for modeling. The machine learning algorithm Boosted Regression Trees (BRT) was selected to analyze the relationships between total C density and the set of environmental predictors because it is suitable for analyzes of non-linear relationships and complex interactions (Assis et al., 2017; Elith et al., 2008).

The model fitted a Gaussian distribution (e.g., Barry and Welsh (2002)) and a cross-validation framework using latitudinal bands (e.g., Assis et al. (2016)) was applied to select the optimal BRT hyperparameters (Elith et al., 2008). This was performed by identifying the model with lower deviance through all parameter combinations of distinct learning rates (0.01, 0.001, and 0.0001), tree complexities (1–6), and number of trees (50–1000, step 50). Individual monotonic responses were forced to all predictors based on the expected effect of the response variable (Assis et al., 2017; Hofner et al., 2011). The ecological significance of models was described by determining the relative importance of each predictor to explain the variation in total C density. The relative importance of predictors was calculated based on the frequency that a variable was selected for splitting during the tree-building process, weighted by its improvement to the overall model (Friedman and Meulman, 2003). In this manner, each variable was scaled as a percentage, with a higher percentage indicating a greater influence on the response. Also, a test was performed to address whether interactions were detected and modelled (Elith et al., 2008). All analyzes were performed in R (R Development Core Team, 2016) and RStudio v.3.6.6 (RStudio Team, 2016).

Quantile regression (QR) was used to establish a quantitative relationship between the dominant driver and conditional quantiles of total C density in forest ecosystems and quantiles of total C density from the dominant driver factor. Quantile regression has the advantage of being able to infer relationships from the edges of scatter graphs (Koenker and Bassett, 1978). For example, the 10th quantile describes a line below which 10% of the observed values are found. Regression quantiles of 0.1, 0.25, 0.5, 0.75 and 0.9, which are often considered as five representative quantile points (Liu et al., 2021), were selected for these analyzes. Details on the theory and use of the quantile regression approach are provided in Appendix 6 (Supplementary Information).

3. Results

3.1. Changes in C storage and C density in vegetation

The total C stored in vegetation and the C density in vegetation increased from 1999 to 2018 (Fig. 2a and b). The mean C storage was 692.66±39.38 Tg and had an annual relative growth rate of 0.71% year^{-1}. The C density increased from 44.54 Mg C ha^{-1} to 48.84 Mg C ha^{-1}, with an increasing trend of 0.22 Mg C ha^{-1} year^{-1} (see Appendix 7, Supporting Information Table S13). The amount of C stored in each layer also increased during the monitoring period, except for the litter layer in 2004–2008. The layers were ranked, from highest mean C storage to lowest, as follows: tree > herb > shrub > litter (Fig. 2a). The amount of C stored in the tree, herb, shrub, and litter layers accounted

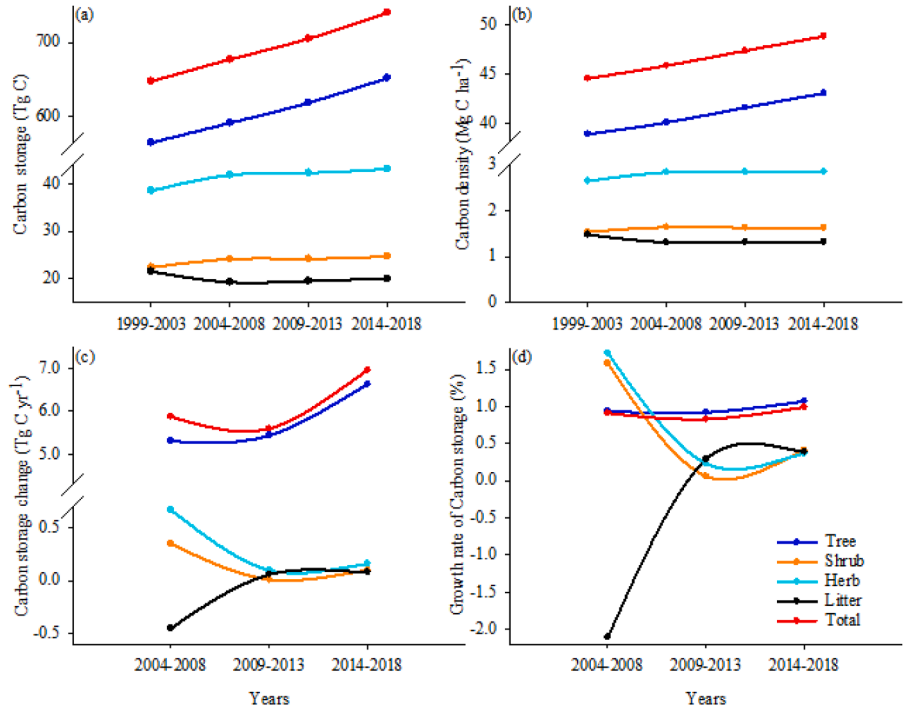

Fig. 2. Carbon (C) storage (a), C density (b), change in C storage (c), and growth rate of C storage (d) in trees, shrubs, herbs, litter, and forest vegetation in the Greater Khingan Mountains from 1999 to 2018.

for 87.65%, 5.99%, 3.45%, and 2.90% of total C stored in vegetation, respectively (see Appendix 8, Supporting Information Table S14). The mean C storage and density were significantly higher in the tree layer than in the other layers (Tables S14 and S15, $p < 0.05$). Of the four layers, the tree layer had the highest mean biomass and C densities (Tables S12 and S15). The C storage and density were around seven times greater in the tree layer than in the other three layers combined (Tables S14 and S15; also see Tables S4–S6).

3.2. Changes of forest vegetation C storage and density in different forest age classes

The area of young and half-mature forests accounted for 80.43% of the total forest area from 1999 to 2018, while the area of near mature, mature, and over mature forests accounted for 9.28, 8.72, and 1.57% of the total forest area, respectively (Fig. 3e). The young and half-mature forests showed gradually increasing C storage from 1999 to 2018, sequestering an average of 1.19 Tg C yr^{-1} and 6.11 Tg C yr^{-1}, respectively, while near mature, mature and over mature forests showed declining C storage, losing C at an average of 0.63 Tg C yr^{-1}, 1.58 Tg C yr^{-1}, and 0.48 Tg C yr^{-1}, respectively (Fig. 3a and c). The C storage differed significantly among forest stand age classes (Table S16, $p < 0.05$). Of the five age classes, the half-mature forests showed the maximum C storage, and over mature forests showed the minimum (Fig. 3a; Table S16). The age classes were ranked, from highest C density to lowest, as follows: mature forests > half-mature forests > near mature forests > over mature forests > young forests (Table S17). C density was significantly lower in young forests than in those of other age classes (Table S17, $p < 0.05$). The C density of each age class gradually increased from the period 1999–2003 to 2014–2018, except for the near mature class (Fig. 3b).

3.3. Changes in forest vegetation C storage and density in different forest types

The dominant species *L. gmelinii* ((7.34±0.18) × 10^6 ha) and *B. platyphylla* ((5.66±0.44) × 10^6 ha) accounted for approximately 49.48% and 38.13% of the total forest area ((14.84±0.25) × 10^6 ha) from 1999 to 2018 (Fig. 4e). C storage differed among forest types and showed substantial variation, with values ranging from 1.45 Tg C to 366.57 Tg C, in the period of 2014–2018 (Fig. 4). The C storage in *L. gmelinii* (366.57 Tg C) was the largest in the latest survey (2014–2018), accounting for 49.5% of the total C storage, followed by *B. platyphylla* (284.08 Tg C) accounting for 38.4% of the total C storage. The C storage in *L. gmelinii* and *Chosenia arbutifolia* decreased in the period of 2004–2008 and increased thereafter. The C storage in *B. platyphylla, P. davidiana, Q. mongolica*, and other forest types increased gradually from 1999 to 2018. However, the C storage in

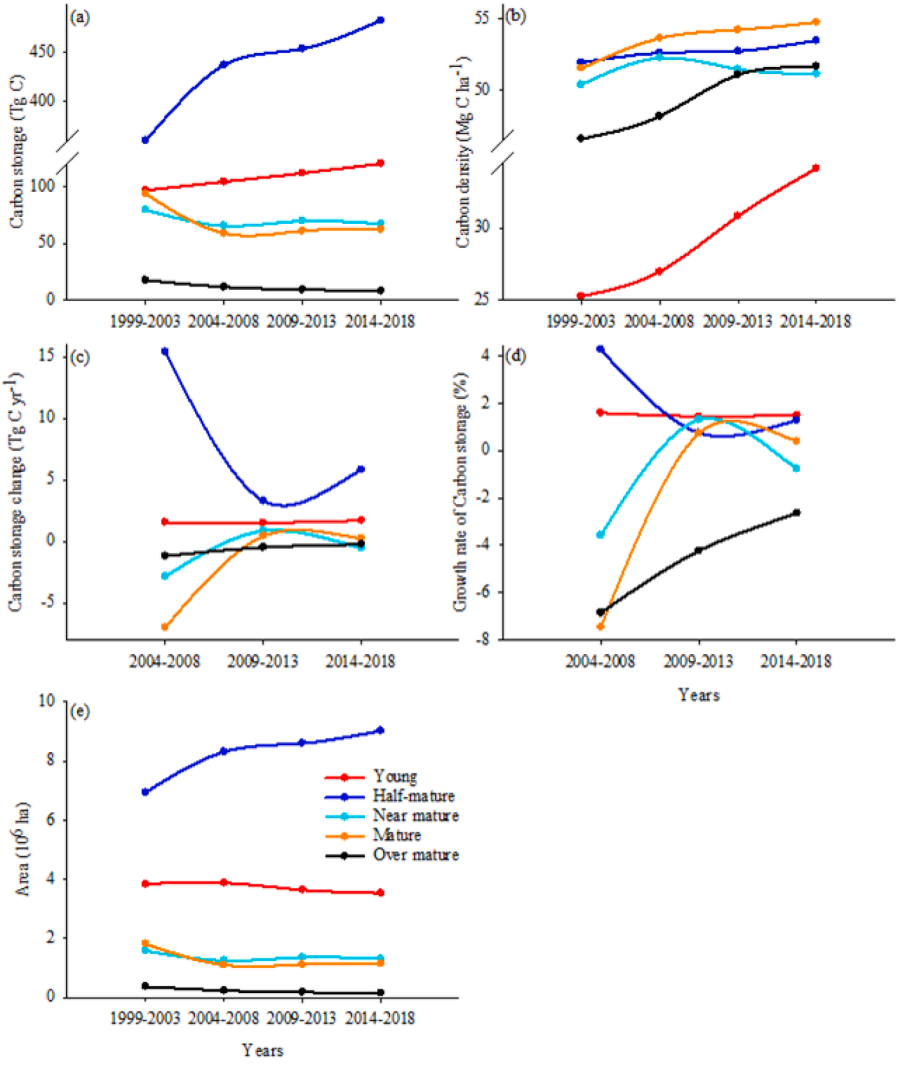

Fig. 3. Carbon (C) storage (a), C density (b), change in C storage (c), growth rate of C storage (d), and area (e) of forest vegetation in different age classes in the Greater Khingan Mountains from 1999 to 2018.

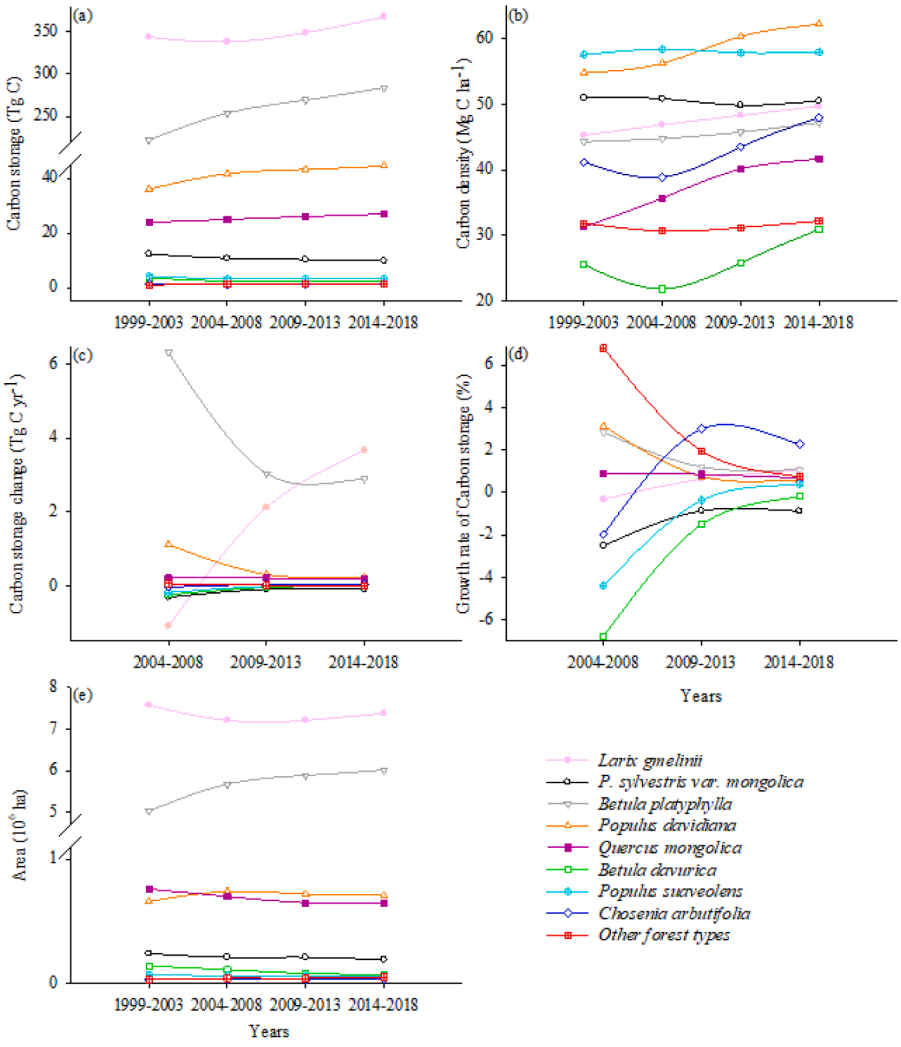

Fig. 4. Carbon (C) storage (a), C density (b), change in C storage (c), growth rate of C storage (d), and area (e) of forest vegetation in different forest types in the Greater Khingan Mountains from 1999 to 2018.

P. sylvestris var. *mongolica, B. davurica*, and *P. suaveolens* decreased gradually from 1999 to 2018 (Fig. 4a). There were considerable differences in C density dynamics over time among forest types in the Greater Khingan Mountains (Table S18, $p < 0.05$). For instance, the C density in *L. gmelinii, B. platyphylla, P. davidiana*, and *Q. mongolica* stands gradually increased over time, whereas in *B. davurica, C. arbutifolia*, and other forest types C density decreased in the period 2004–2008 and then increased thereafter. Similarly, the C density in *P. sylvestris* var. *mongolica* stands decreased from 1999 to 2013 and then slightly increased after 2014 (Fig. 4b). Among all the forest types, *P. davidiana* stands had the highest C density, peaking in the latest survey at 62.2 Mg C ha^{-1} (Fig. 4b). The C density in *P. davidiana* forests in the latest survey was only 13.2% higher than that in the same forest type at the beginning of the monitoring period 15 years before. However, it was more than double of *B. davurica* forests, which had the lowest C density in the latest survey (Fig. 4b).

3.4. Effects of environmental variables on total C density in the forest ecosystem

The model using the best set of hyperparameters (learning rate: 0.01; tree complexity: 2; number of trees: 1000) explained a large proportion of the deviance of 0.54±0.02 Mg C ha^{-1} between the observed and predicted values (Fig. S3). The predictors mean annual temperature (MAT; °C) and mean annual precipitation (MAP; mm) largely explained the variation in total C density, including C density in soils. The relative importance of MAT and MAP was >13%. The combined importance of the other five parameters — precipitation of warmest quarter (BIO18; mm), temperature seasonality (BIO4; °C), aridity index (AI), precipitation seasonality (BIO15; mm) and total phosphorus (TP; g kg^{-1}) — was 43.9% (Fig. 5). Only non-significant and weak (<1%) interactions among parameters were detected (Table S10).

There was a significant relationship between total C density and MAT ($R^2 = 0.78$, $p < 0.001$). The values of total C density ranged from 59.1 Mg C ha^{-1} at a MAT of −4.8 °C to 235.2 Mg C ha^{-1} at a MAT of −2.3 °C, with a mean (± standard error) value of 111.3 ± 2.9 Mg C ha^{-1}. Each estimated quantile curve comprised two linear segments with one inflection point, and was statistically significant at the 0.05 level (Fig. 6 and Table S11). In the case of the lower quantiles (τ= 0.1 and 0.25), the inflection point was MAT = −2.1 °C. This fact indicates that the total C density of forest ecosystems increased with increasing MAT when the MAT was lower than −2.1 °C (2.0 Mg C ha^{-1}/1 °C for τ= 0.1 and 2.7 Mg C ha^{-1}/1 °C for τ= 0.25), but it decreased with increasing MAT when the MAT was higher than −2.1 °C (1.4 Mg C ha^{-1}/1 °C for τ= 0.1 and 2.4 Mg C ha^{-1}/1 °C for τ= 0.25). For the mid-level quantile (τ= 0.5), when MAT increased by 1 °C, the total forest C density increased by 3.7 Mg C ha^{-1}. However, beyond the threshold of −2.4 °C, when MAT increased by 1 °C, the total forest C density decreased by 2.8 Mg C ha^{-1}. Finally, we considered the higher quantiles (τ= 0.75 and 0.9) that correspond to a high total C density. In these cases, the inflection points dropped to

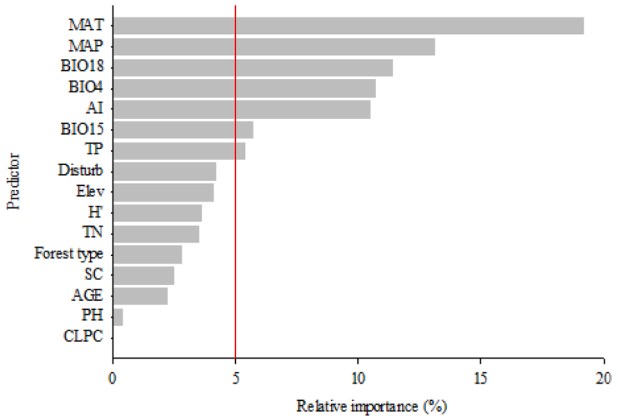

Fig. 5. Relative importance (%) of all variables for the model of total carbon (C) density of forest ecosystems (including forest vegetation and soil C density, Mg C ha^{-1}) with mean annual temperature (MAT; °C), mean annual precipitation (MAP; mm), precipitation of warmest quarter (BIO18; mm), temperature seasonality (BIO4; °C), aridity index (AI), precipitation seasonality (BIO15; mm), total phosphorus (TP; g kg^{-1}), management and disturbance (Disturb), elevation (Elev; m), Shannon-Wiener diversity index (H'), total nitrogen (TN, g kg^{-1}), forest type, sand content (SC, mass%), stand age (AGE, year), pH (soil) and clay content (CLPC; mass%). Red line indicates 5% relative importance to the model.

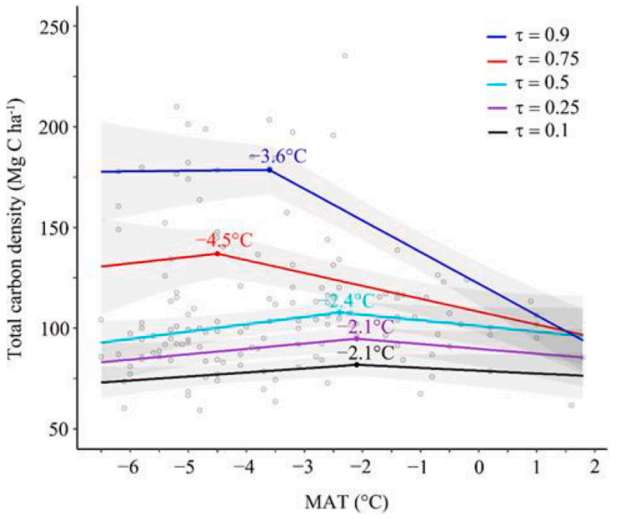

Fig. 6. Estimates of piecewise-linear quantile curves determining relationship between total carbon (C) density of forest ecosystems (including forest vegetation and soil C density, Mg C ha^{-1}) and mean annual temperature (MAT, °C) in the Greater Khingan Mountains using a total variation roughness penalty at τ = 0.1, 0.25, 0.5, 0.75, and 0.9. Gray circles (n = 149) represent measured values of total C density of forest ecosystems at different sites across the Greater Khingan Mountains with the corresponding measured MAT.

−4.5 °C and −3.6 °C, suggesting that in a forest ecosystem with high total C density, MAT may have a small positive effect when it is lower than the inflection point but a large negative effect when it is above the threshold.

Regarding other environmental predictors, the spatial pattern of the total C density showed a strong correlation with MAP, BIO18, and BIO4 (R^2 = 0.30−0.42, $p < 0.05$; Fig. S4). The total C density in the forest ecosystems decreased with increasing precipitation (MAP and BIO18), but decreased at a higher rate in the regions with increasing BIO18 than those with increasing MAP. The total C density in forest ecosystems was more strongly negatively correlated with BIO18 than with MAP (3.3 Mg C ha^{-1}/10 mm vs. 2.5 Mg C ha^{-1}/10 mm; Fig. S4a and b). By contrast, we found that the total C density showed a positive relationship with BIO4. In this case, when BIO4 increased by 1 °C, the total C density of forest ecosystems increased by 0.1 Mg C ha^{-1} (Fig. S4c). These results showed that the total C density of forest ecosystems exhibits various feedbacks to climatic variables.

4. Discussion

Our results show that young and half-mature forests contribute much to the C storage in these forests: young stands because of their expansion over time, and mature forests because of their high C density. However, our results also show that temperature is the main factor influencing C density. Expected temperature increases, combined with forest stand dynamics, will reinforce the dynamic nature of C density and storage, as discussed in detail in the following sections.

4.1. C storage and density in forest vegetation

Our estimate of C storage in vegetation in the boreal forests of the Greater Khingan Mountains was 740.13 Tg C in 2018. Tang et al. (2018) reported that China's forest vegetation C storage was 13.01 Pg C. Hence, C storage in the Greater Khingan Mountains in 2018 accounted for approximately 5.7% of China's C storage. In 2018, the C density in the tree layer of forests in the Greater Khingan Mountains was lower than average value for all China's forests (43.0 vs. 55.7 Mg C ha^{-1}; (Tang et al., 2018). The main reason for this difference may be the age structure of the forests in the Greater Khingan Mountains—the area of young forests, with significantly low C density ($p < 0.05$; Fig. 3b), accounted for approximately 30% of the total forest area in the latest survey (2014–2018)—and a minor reason may be the influence of human disturbance (Fang et al., 2001). Differences could also be a consequence of previous studies lacking direct inventory data, or even if direct inventory data were available, the sample size used to characterize those forests was insufficient for C storage estimation compared with China's national-scale inventory data.

The dominance of young forests reflects the land-use history of the area. That is, there was long-term and high-intensity deforestation before the "Grain for Green" program and the Natural Forest Protection project in 1998, which generated the majority of young forests (Duan et al., 2017; Lu et al., 2018). Additionally, wildfires are the major disturbance in boreal forests (Payette, 1992), and result in stands dominated by young age classes (Larsen, 1997). C storage in young and half-mature forests gradually increased during the monitoring period, mainly driven by their expansion in forest area. If nothing is done to reduce disturbances, then they will become more frequent and the ratio of young to mature forests will increase. This process is directly linked to forest densification already observed in other southern Eurasian boreal forests (Kharuk et al., 2010).

In addition, litter C storage decreased in the period of 2004–2008 compared with that in previous years. This may be because the forests in this region have been subject to frequent surface forest fires with short fire return intervals (Cai et al., 2013; Tao et al., 2013), resulting in C losses in the litter layer. Other possible interpretations of the results are changes in the age class structure (distribution) caused by harvesting in this study area, which has resulted in stands dominated by young and half mature age classes. Compared with mature and over mature stands, young stands dominated by *L. gmelinii* and *B. platyphylla* had relatively small litter layers (Table S6), because of low rates of litter production by juvenile trees (Karhu et al., 2011). Furthermore, overgrazing can significantly reduce litter inputs and impede forest regeneration, as seen in Mongolian boreal forests (Tsogtbaatar, 2004). Russian boreal forests in the Far East region are facing similar challenges (Shvidenko, 2011). To enhance C storage in vegetation, the Chinese government has prohibited commercial logging in natural forests since April 1st, 2015, and is also closing hillsides to facilitate afforestation and to establish higher litter and shrub cover in these mountains.

Among all the forest age classes, young forests had the lowest C density, and mature forests had the highest. This pattern, plus the large proportion of young forests, suggests that forests in this region have a high potential to sequester and store more C in the future. Other things being equal, mature forests are characterized by low productivity, and hence, a low C sequestration capacity (Bhatti et al., 2002; Yu et al., 2011). Therefore, our results highlight that information on age class structure must be considered to obtain an accurate estimate of C storage at regional scales, particularly in southeastern Eurasian boreal forests.

The proportions of C stored in *L. gmelinii* and *B. platyphylla* stands in the Greater Khingan Mountains accounted for 87.57% of the total C storage in forest vegetation. Such a high proportion of C storage by these two species, primarily driven by their high proportion of forest area, is not surprising—they are the dominant species in the region (Liu et al., 2020b). However, these stands were not necessarily the ones with the highest C density. In fact, our results suggest that *P. davidiana* and *P. suaveolens* (broadleaf species), and *P. sylvestris* var. *mongolica* and *L. gmelinii* (conifers) could be the preferred species for afforestation and transformation of secondary forest stands aiming to maximize C density, because the particular features of their tissues (Zhang et al., 2009) and the strong adaptability of these species to low temperature. In addition, these species show efficient utilization of water from melting permafrost during the hot and dry summer, resulting in higher C storage than that of the other tree species (Shi et al., 2010; above 47.52±1.91 Mg C ha^{-1}). Hence, our first initial hypothesis on C density depending on structural forest features (age, species composition) can be accepted.

Observed differences among forest types can also have implications for forest dynamics. For example, C density increased much faster in *P. davidiana* forest than in *B. davurica* forest. These changes probably reflect a beneficial effect of climate warming on poplar growth rates (Yun et al., 2021), but also increased growth of the understory in older poplar stands (Table S5), likely because of increased mortality of the overstory. However, poplar forests are also more prone to damage by increased weather variability of winter months under climate change and are affected with different intensity by defoliators common to both poplar and birch (Man et al., 2014). As a result, the expected dynamics of these forests could consist in periods of relative stability followed by abrupt non-linear shifts, as already reported for poplar/birch sites in boreal Canadian forests (Van Bogaert et al., 2009). Multi-temporal field studies on C storage and density, such as the present study, can also inform forest management and C sequestration management models (Li et al., 2022b).

4.2. Effects of environmental factors on total C density in forest ecosystems

C density in boreal forests is affected by climate, soil type, and plant species, which control the processes of primary production and decomposition (Bhatti et al., 2002). When compared with climate variables, soil variables such as clay content and pH had the weakest ability to explain the variation in total C density because the soil type in the Greater Khingan Mountains is mostly a dark brown forest soil (Liu et al., 2020b), and its formation is closely associated with permafrost conditions (Baumann et al., 2009; Xu, 1998). Boreal ecosystems have low temperatures, and the permafrost reduces soil drainage and creates a high moisture content in the seasonally thawed active layer (i.e. the gleying process of soil). Consequently, the available soil space is reduced, and this hinders the development of large microbial communities. In turn, this reduces nutrient circulation in decomposing organic matter and leads to much slower tree growth and C accumulation rates (Jarvis and Linder, 2000; Waelbroeck, 1993).

Other variables with low relative importance (< 5%) in explaining the variation in total C density were age structure, forest type, and disturbance intensity. This result may indicate that even if there are clear structural differences in C density among forest ages, this influence is much weaker than that of climate, the main growth limiting factor at these sites. The low importance of disturbances to explaining the variation in total C density may be because relatively small areas are affected by sudden disturbances (Tao et al., 2013) that produce detectable changes in canopy cover. This low influence of management could also indicate that the Natural Forest Protection Plan introduced in the region in 1998 has been effective in reducing human impacts on forest C stocks. Additionally, not all variability was explained in our models, likely because of additional drivers, as well as stochastic variability, which can be divided among monitoring period, sample plot, and within-sample plot components (Calama and Montero, 2005).

A non-significant relationship was observed between total forest C density and AI, BIO15, and TP ($R^2 < 0.1, p > 0.05$; Fig. S4d–f), indicating that each of these variables has a relatively small importance (see Appendix 9 in the Supplementary Information for details), which was also verified by the BRT model, highlighting that MAT was the most important environmental driver of total C density, followed by MAP (Fig. 5). These findings are consistent with those of Guo et al. (2019), who concluded that MAT exerted the strongest effect on boreal forests. Another study found that MAT directly affects C pools in boreal forests by influencing stem taper (Liu et al., 2020a). Both MAT and MAP have direct effects on species distribution (a major driver of structural C density) and indirect effects on forest growth, both of which affect mortality, and subsequently, dominant stand age. For example, raising temperatures have led to large growth declines and lower C density achieved in young Korean pine trees, but have had little effect on older trees. This is because Korean pine is a shallow-rooted tree species. When root systems are underdeveloped in young ages, Korean pine is more sensitive to water stress caused by low MAP, and this is exacerbated by increasing temperature (Wang et al., 2019). Kauppi and Posch (1985) also found that temperature was a very important ecological factor for boreal forests mainly because there is a rapid increase in tree mortality as temperatures increase. It is widely accepted that Earth's global surface temperature has increased and the largest increase has occurred in boreal forests (Hansen et al., 1996). Hence, increased temperatures will change the composition, distribution range, and current mosaic structure of boreal forests (Allen et al., 2010; Soja et al., 2007).

Nevertheless, we detected a non-linear relationship between MAT and total C density, supporting our second initial hypothesis. In contrast, Liu et al. (2014c) predicted that total C density would have a linear relationship with MAT in boreal coniferous forests. Interestingly, the MAT thresholds in which the MAT influence changed from positive to negative depended on the value of total C density. Using a quantile regression (Fig. 6), we identified a tendency for forests with the highest C density to have lower MAT values as thresholds, implying that those forests with more developed tree, shrub, and litter layers (usually productive mature stands or old-growth forests) will be negatively impacted earlier by raising global temperatures than young or non-productive stands. Such result highlights that temperature should be considered when studying past and predicting future responses of total C density to climate change or when estimating total C density, but also that assuming linear relationships may cause misestimates of C pools. Such a relationship also calls attention to the importance of studies on total C density at regional scales to improve the accuracy of estimations. For example, Tang et al. (2018) found a significant negative effect of MAT on the total C density, but it had a higher decreasing rate in regions where the MAP was 400 mm or less, such as parts of the Greater Khingan Mountains and most of the central-eastern Eurasian boreal forests. Guo et al. (2019) identified a MAT value of 0 °C as the threshold for changes in total C density of boreal forests in 2070 under three emission scenarios (RCP2.6, RCP4.5, and RCP8.5). Those findings are consistent with our results of non-linearity, although with different numeric relationships between MAT and total forest C density.

We found that an increase in total C density in forests where MATs were below the identified thresholds was followed by a decrease in total C density in forests where MATs were above the thresholds. Although the magnitude of the increases differed (Table S11, Supplementary

Information), the relative changes had a similar pattern at different quantile points of the total C density conditional distribution (Fig. 6). A possible reason for this C density response to temperature is that *L. gmelinii* is able to adapt to cold temperatures and efficiently use water from the thawing permafrost during summer (Xu, 1998). Another possible reason could be the acceleration of the nitrogen cycle due to increased temperature, which would facilitate litter decomposition and result in increased C density in the trees (Lo et al., 2019; Melillo et al., 2011). It is also possible that, in *L. gmelinii* forests, a moderate increase in temperature promotes biomass and productivity, but higher temperatures quickly become the limiting factor for growth. This will be particularly important because no significant increase in MAP is expected for this region under climate change (Shvidenko, 2011).

When the temperature exceeds a threshold, warmer conditions cause water stress that negatively affects tree growth, and ultimately leads to a rapid increase in tree mortality rates in boreal forests (Chaste et al., 2019; Girardin et al., 2016). For those stands, increased mortality, accompanied by little growth gain under warming temperatures, leads to large decreases in net biomass (Chen et al., 2016). In addition, soil C can decompose faster, reducing soil C density. The effects of MAT on total C density may be highly dependent on the spatial scale because of topographical effects. However, even though the spatial scale of our study was regional, we are confident that our C estimations are more exhaustive than those calculated only from national inventory data, and that they are representative for this forest area at the southern limits of eastern Eurasian boreal forests.

5. Conclusions

We analyzed C storage in forests in the Greater Khingan Mountains in China. Vegetation C storage depended on stand age and forest species structure. Young and half-mature forests together accounted for 80.43% of the total forest area during the monitoring period. Young forests had the lowest C density, while mature forests had the highest C density. This implies that the forests of the Greater Khingan Mountains will play important roles as potential C sinks to store C in the future. C storage rates differed widely among forest types, and were the highest in *P. davidiana* forests. The MAT was the main factor controlling total ecosystem C density. However, total C density increased with increasing MAT before an inflection point was reached in the -4.5 to -2.1 °C range, and thereafter decreased with increasing MAT. Therefore, the maximum total C density was at these temperature thresholds, in a range encompassing the local MATs. We were able to determine the quantitative relationship between the total C density and its dominant driver at different rates of change. Our results suggest that the ecosystem can adapt to maximize C density at the current regional average temperature, indicating that anthropogenic climate change might affect the ability of these forests to store and maintain high C densities.

CRediT authorship contribution statement

Yang Liu: Writing – original draft. **Ralph Trancoso:** Formal analysis. **Qin Ma:** Writing – review & editing. **Philippe Ciais:** Writing – review & editing. **Lidiane P. Gouvêa:** Methodology. **Chaofang Yue:** Formal analysis. **Jorge Assis:** Methodology. **Juan A. Blanco:** Conceptualization, Supervision, Writing – review & editing.

Declaration of Competing Interest

The authors declare that they have no known competing financial interests or personal relationships that could have appeared to influence the work reported in this paper.

Data availability

Data will be made available on request.

Acknowledgments

We thank Qiang Ren from Jinhe Forestry Bureaus of Inner Mongolia, Changlei Wei from Greater Khingan Mountains A&F Academy, and Qibao Zhang from Inner Mongolia Agricultural University for providing some of the data used in this study. We greatly appreciate the anonymous reviewers' valuable comments and suggestions on the manuscript. This study was funded by the National Natural Science Foundation of China (32160363), the Natural Science Foundation of Inner Mongolia Autonomous Region (2021MS03096), the Science and Technology Planning Program of Inner Mongolia Autonomous Region (2020GG0067), the Foundation for Science and Technology (FCT) of Portugal through projects UIDB/04326/2020, UIDP/04326/2020, LA/P/0101/2020, PTDC/BIA-CBI/6515/2020, and the Individual Call to Scientific Employment Stimulus 2022.00861. Open access funding provided by the Public University of Navarre.

Supplementary materials

Supplementary material associated with this article can be found, in the online version, at doi:10.1016/j.agrformet.2023.109519.

References

Allen, C.D., Macalady, A.K., Chenchouni, H., Bachelet, D., McDowell, N., Vennetier, M., Cobb, N., 2010. A global overview of drought and heat-induced tree mortality reveals emerging climate change risks for forests. For. Ecol. Manag. 259 (4), 660–684. https://doi.org/10.1016/j.foreco.2009.09.001.

Assis, J., Berecibar, E., Claro, B., Alberto, F., Reed, D., Raimondi, P., Serrão, E.A., 2017. Major shifts at the range edge of marine forests: the combined effects of climate changes and limited dispersal. Sci. Rep. 7 (1), 44348. https://doi.org/10.1038/srep44348.

Assis, J., Coelho, N.C., Lamy, T., Valero, M., Alberto, F., Serrão, E.Á., 2016. Deep reefs are climatic refugia for genetic diversity of marine forests. J. Biogeogr. 43 (4), 833–844. https://doi.org/10.1111/jbi.12677.

Bai, X., Zhang, X., Li, J., Duan, X., Jin, Y., Chen, Z., 2019. Altitudinal disparity in growth of Dahurian larch (Larix gmelinii Rupr.) in response to recent climate change in northeast China. Sci. Total Environ. 670, 466–477. https://doi.org/10.1016/j.scitotenv.2019.03.232.

Barry, S.C., Welsh, A.H., 2002. Generalized additive modelling and zero inflated count data. Ecol. Model. 157 (2), 179–188. https://doi.org/10.1016/S0304-3800(02)00194-1.

Batjes, N.H., 2015. World soil property estimates for broad-scale modelling (WISE30sec, ver. 1.0). Report 2015/01, ISRIC-World Soil Information, Wageningen, Netherlands (with data set, available at https://www.isric.org).

Baumann, F., He, J.S., Schmidt, K., Kühn, P., Scholten, T., 2009. Pedogenesis, permafrost, and soil moisture as controlling factors for soil nitrogen and carbon contents across the Tibetan Plateau. Glob. Chang. Biol. 15 (12), 3001–3017. https://doi.org/10.1111/j.1365-2486.2009.01953.x.

Bhatti, J.S., Apps, M.J., Jiang, H., 2002. Influence of nutrients, disturbances and site conditions on carbon stocks along a boreal forest transect in central Canada. Plant Soil 242 (1), 1–14. https://doi.org/10.1023/A:1019670619316.

Bonan, G.B., 2008. Forests and climate change: forcings, feedbacks, and the climate benefits of forests. Science 320 (5882), 1444–1449. https://doi.org/10.1126/science.1155121.

Bonan, G.B., Cleve, K.V., 1992. Soil temperature, nitrogen mineralization, and carbon source–sink relationships in boreal forests. Can. J. For. Res. 22 (5), 629–639. https://doi.org/10.1139/x92-084.

Bradshaw, C.J.A., Warkentin, I.G., Sodhi, N.S., 2009. Urgent preservation of boreal carbon stocks and biodiversity. Trends Ecol. Evol. 24 (10), 541–548. https://doi.org/10.1016/j.tree.2009.03.019.

Brown, A.H., Johnson, Z.B., Chewning, J.J., Brown, C.J., 1988. Relationships among absolute growth rate, relative growth rate and feed conversion during postweaning feedlot performance tests. J. Anim. Sci. 66 (10), 2524–2529. https://doi.org/10.2527/jas1988.66102524x.

Bu, R., He, H.S., Hu, Y., Chang, Y., Larsen, D.R., 2008. Using the LANDIS model to evaluate forest harvesting and planting strategies under possible warming climates in Northeastern China. For. Ecol. Manag. 254 (3), 407–419. https://doi.org/10.1016/j.foreco.2007.09.080.

Cai, W., Yang, J., Liu, Z., Hu, Y., Weisberg, P.J., 2013. Post-fire tree recruitment of a boreal larch forest in Northeast China. For. Ecol. Manag. 307, 20–29. https://doi.org/10.1016/j.foreco.2013.06.056.

Calama, R., Montero, G., 2005. Multilevel linear mixed model for tree diameter increment in stone pine (Pinus pinea): a calibrating approach. Silva Fenn 39 (1), 37–54. https://doi.org/10.14214/sf.394.

Cannell, M.G.R., Milne, R., 1995. Carbon pools and sequestration in forest ecosystems in Britain. Forestry 68 (4), 361–378. https://doi.org/10.1093/forestry/68.4.361.

Chaste, E., Girardin, M.P., Kaplan, J.O., Bergeron, Y., Hély, C., 2019. Increases in heat-induced tree mortality could drive reductions of biomass resources in Canada's

managed boreal forest. Landscape Ecol. 34 (2), 403–426. https://doi.org/10.1007/s10980-019-00780-4.
Chen, H.Y.H., Luo, Y., Reich, P.B., Searle, E.B., Biswas, S.R., 2016. Climate change-associated trends in net biomass change are age dependent in western boreal forests of Canada. Ecol. Lett. 19 (9), 1150–1158. https://doi.org/10.1111/ele.12653.
Chen, L., Guan, X., Li, H.M., Wang, Q.K., Zhang, W.D., Yang, Q.P., Wang, S.L., 2019. Spatiotemporal patterns of carbon storage in forest ecosystems in Hunan Province. China. For. Ecol. Manag. 432, 656–666. https://doi.org/10.1016/j.foreco.2018.09.059.
Crowther, T.W., Todd-Brown, K.E.O., Rowe, C.W., Wieder, W.R., Carey, J.C., Machmuller, M.B., Bradford, M.A., 2016. Quantifying global soil carbon losses in response to warming. Nature 540 (7631), 104–108. https://doi.org/10.1038/nature20150.
De Marco, P.J., Nóbrega, C.C., 2018. Evaluating collinearity effects on species distribution models: an approach based on virtual species simulation. PLoS One 13 (9), e0202403. https://doi.org/10.1371/journal.pone.0202403.
DFPRC, 2014. Statistics of China's Forest Resources (2009-13). Department of Forestry of PRC, Beijing, China.
Dixon, R.K., Solomon, A.M., Brown, S., Houghton, R.A., Trexier, M.C., Wisniewski, J., 1994. Carbon pools and flux of global forest ecosystems. Science 263 (5144), 185–190. https://doi.org/10.1126/science.263.5144.185.
Duan, L., Man, X., Kurylyk, B.L., Cai, T., Li, Q., 2017. Distinguishing streamflow trends caused by changes in climate, forest cover, and permafrost in a large watershed in northeastern China. Hydrol. Process. 31 (10), 1938–1951. https://doi.org/10.1002/hyp.11160.
Editorial Committee for Vegetation of China, 1980. Vegetation of China. Science Press, Beijing, China.
Elith, J., Leathwick, J.R., Hastie, T., 2008. A working guide to boosted regression trees. J. Anim. Ecol. 77 (4), 802–813. https://doi.org/10.1111/j.1365-2656.2008.01390.x.
Fang, J., Chen, A., Peng, C., Zhao, S., Ci, L., 2001. Changes in forest biomass carbon storage in China between 1949 and 1998. Science 292 (5525), 2320–2322. https://doi.org/10.1126/science.1058629.
FAO, 2020. Global Forest Resources Assessment 2020: Main Report. Food and Agriculture Organization of the United Nations, Rome, Italy. https://doi.org/10.4060/ca9825en.
Flombaum, P., Sala, O.E., 2008. Higher effect of plant species diversity on productivity in natural than artificial ecosystems. PNAS 105 (16), 6087–6090. https://doi.org/10.1073/pnas.0704801105.
Friedman, J.H., Meulman, J.J., 2003. Multiple additive regression trees with application in epidemiology. Stat. Med. 22 (9), 1365–1381. https://doi.org/10.1002/sim.1501.
Girardin, M.P., Hogg, E.H., Bernier, P.Y., Kurz, W.A., Guo, X.J., Cyr, G., 2016. Negative impacts of high temperatures on growth of black spruce forests intensify with the anticipated climate warming. Glob. Chang. Biol. 22 (2), 627–643. https://doi.org/10.1111/gcb.13072.
Guo, Y., Peng, C., Trancoso, R., Zhu, Q., Zhou, X., 2019. Stand carbon density drivers and changes under future climate scenarios across global forests. For. Ecol. Manag. 449, 117463 https://doi.org/10.1016/j.foreco.2019.117463.
Hansen, J., Ruedy, R., Sato, M., Reynolds, R., 1996. Global surface air temperature in 1995: return to pre-Pinatubo level. Geophys. Res. Lett. 23 (13), 1665–1668. https://doi.org/10.1029/96 gl01040.
Hofner, B., Müller, J., Hothorn, T., 2011. Monotonicity-constrained species distribution models. Ecology 92 (10), 1895–1901. https://doi.org/10.1890/10-2276.1.
Holland, E.A., Brown, S., 1999. North American carbon sink. Science 283 (5409), 1815. https://doi.org/10.1126/science.283.5409.1815a. -1815.
Houghton, J.T., Jenkins, G.J., Ephraums, J.J., 1990. Climate Change: The IPCC Scientific Assessment. Cambridge University Press, Cambridge.
Houghton, R.A., Roy, J., Saugier, B., Mooney, H.A., 2001. Global terrestrial productivity and carbon balance. Terrestrial Global Productivity. Academic Press, San Diego, California, pp. 499–520.
Hu, L., Fan, W., Ren, H., Liu, S., Cui, Y., Zhao, P., 2018. Spatiotemporal dynamics in vegetation GPP over the Great Khingan Mountains using GLASS products from 1982 to 2015. Remote Sens. 10 (3), 488. https://doi.org/10.3390/rs10030488.
Imbert, J.B., Blanco, J.A., Candel-Pérez, D., Lo, Y.H., González de Andrés, E., Yeste, A., Chang, S.C., Venkatramanan, V., Shah, S., Prasad, R., 2021. Synergies between climate change, biodiversity, ecosystem function and services, indirect drivers of change and human well-being in forests. Exploring Synergies and Trade-Offs between Climate Change and the Sustainable Development Goals. Springer, Singapore, pp. 263–320.
IPCC, Eggleston, S., Buendia, L., Miwa, K., Ngara, T., Tanabe, K., 2006. 2006 IPCC Guidelines for National Greenhouse Gas Inventories, Prepared by the National Greenhouse Gas Inventories Programme. IGES, Hayama, Japan (accessed 13 January 2023).
Jarvis, P., Linder, S., 2000. Constraints to growth of boreal forests. Nature 405 (6789), 904–905. https://doi.org/10.1038/35016154.
Jobbágy, E.G., Jackson, R.B., 2000. The vertical distribution of soil organic carbon and its relation to climate and vegetation. Ecol. Appl. 10 (2), 423–436. https://doi.org/10.1890/1051-0761(2000)010[0423:TVDOSO]2.0.CO;2.
Johnson, W.C., Sharpe, D.M., 1983. The ratio of total to merchantable forest biomass and its application to the global carbon budget. Can. J. For. Res. 13 (3), 372–383. https://doi.org/10.1139/x83-056.
Karhu, K., Wall, A., Vanhala, P., Liski, J., Esala, M., Regina, K., 2011. Effects of afforestation and deforestation on boreal soil carbon stocks—comparison of measured C stocks with Yasso07 model results. Geoderma 164 (1), 33–45. https://doi.org/10.1016/j.geoderma.2011.05.008.
Karjalainen, T., 1996. The carbon sequestration potential of unmanaged forest stands in Finland under changing climatic conditions. Biomass Bioenergy 10 (5), 313–329. https://doi.org/10.1016/0961-9534(95)00123-9.
Kauppi, P., Posch, M., 1985. Sensitivity of boreal forests to possible climatic warming. Clim. Chang. 7 (1), 45–54. https://doi.org/10.1007/BF00139440.
Kharuk, V.I., Ranson, K.J., Im, S.T., Vdovin, A.S., 2010. Spatial distribution and temporal dynamics of high-elevation forest stands in southern Siberia. Glob. Ecol. Biogeogr. 19 (6), 822–830. https://doi.org/10.1111/j.1466-8238.2010.00555.x.
Kirilenko, A.P., Sedjo, R.A., 2007. Climate change impacts on forestry. PNAS 104 (50), 19697–19702. https://doi.org/10.1073/pnas.0701424104.
Koenker, R., Bassett, J.G., 1978. Regression quantiles. Econom. J. Econ. Soc. 102, 231–243. https://doi.org/10.1016/j.energy.2016.02.025.
Larsen, C.P.S., 1997. Spatial and temporal variations in boreal forest fire frequency in northern Alberta. J. Biogeogr. 24 (5), 663–673. https://doi.org/10.1111/j.1365-2699.1997.tb00076.x.
Li, F., Liu, Y., Zhang, C., Sa, R., Tie, N., 2022a. Precipitation and understory vegetation diversity drive variations in soil organic carbon density: results from field surveys and satellite data of two different periods in the Greater Khingan Mountains of northeast China. Appl. Ecol. Environ. Res. 20 (3), 2303–2328. https://doi.org/10.15666/aeer/2003_23032328.
Li, W., Jiang, Y., Dong, M., Du, E., Zhou, Z., Zhao, S., Xu, H., 2020. Diverse responses of radial growth to climate across the southern part of the Asian boreal forests in northeast China. For. Ecol. Manag. 458, 117759 https://doi.org/10.1016/j.foreco.2019.117759.
Li, Y., Luo, T., Li, S., Liu, B., 2022b. Modeling optimal forest rotation age for carbon sequestration in the Great Khingan Mountains of Northeast China. Forests 13 (6), 838. https://doi.org/10.3390/f13060838.
Liu, H., Park Williams, A., Allen, C.D., Guo, D., Wu, X., Anenkhonov, O.A., Badmaeva, N. K., 2013. Rapid warming accelerates tree growth decline in semi-arid forests of Inner Asia. Glob. Chang. Biol. 19 (8), 2500–2510. https://doi.org/10.1111/gcb.12217.
Liu, H., Ren, H., Hui, D., Wang, W., Liao, B., Cao, Q., 2014a. Carbon stocks and potential carbon storage in the mangrove forests of China. J. Environ. Manag. 133, 86–93. https://doi.org/10.1016/j.jenvman.2013.11.037.
Liu, Q., Meng, S., Zhou, H., Zhou, G., Li, Y., 2017. Tree Volume Tables of China. China Forestry Press, Beijing, China.
Liu, Y., Blanco, J.A., Wei, X., Kang, X., Wang, W., Guo, Y., 2014b. Determining suitable selection cutting intensities based on long-term observations on aboveground forest carbon, growth, and stand structure in Changbai Mountain, Northeast China. Scand. J. For. Res. 29 (5), 436–454. https://doi.org/10.1080/02827581.2014.919352.
Liu, Y., Lin, B., Xu, B., 2021. Modeling the impact of energy abundance on economic growth and CO_2 emissions by quantile regression: evidence from China. Energy 227, 120416. https://doi.org/10.1016/j.energy.2021.120416.
Liu, Y., Trancoso, R., Ma, Q., Yue, C., Wei, X., Blanco, J.A., 2020a. Incorporating climate effects in Larix gmelinii improves stem taper models in the Greater Khingan Mountains of Inner Mongolia, northeast China. For. Ecol. Manag. 464, 118065 https://doi.org/10.1016/j.foreco.2020.118065.
Liu, Y., Yu, G., Wang, Q., Zhang, Y., 2014c. How temperature, precipitation and stand age control the biomass carbon density of global mature forests. Glob. Ecol. Biogeogr. 23 (3), 323–333. https://doi.org/10.1111/geb.12113.
Liu, Y., Yue, C., Wei, X., Blanco, J.A., Trancoso, R., 2020b. Tree profile equations are significantly improved when adding tree age and stocking degree: an example for Larix gmelinii in the Greater Khingan Mountains of Inner Mongolia, northeast China. Eur. J. For. Res. 139 (3), 443–458. https://doi.org/10.1007/s10342-020-01261-z.
Liu, Z., Yang, J., Chang, Y., Weisberg, P.J., He, H.S., 2012. Spatial patterns and drivers of fire occurrence and its future trend under climate change in a boreal forest of Northeast China. Glob. Chang. Biol. 18 (6), 2041–2056. https://doi.org/10.1111/j.1365-2486.2012.02649.x.
Lo, Y.H., Blanco, J.A., González de Andrés, E., Imbert, J.B., Castillo, F.J., 2019. CO_2 fertilization plays a minor role in long-term carbon accumulation patterns in temperate pine forests in the southwestern Pyrenees. Ecol. Model. 407, 108737 https://doi.org/10.1016/j.ecolmodel.2019.108737.
Lu, F., Hu, H., Sun, W., Zhu, J., Liu, G., Zhou, W., Yu, G., 2018. Effects of national ecological restoration projects on carbon sequestration in China from 2001 to 2010. PNAS 115 (16), 4039–4044. https://doi.org/10.1073/pnas.1700294115.
Ma, Z., Peng, C., Zhu, Q., Chen, H., Yu, G., Li, W., Zhang, W., 2012. Regional drought-induced reduction in the biomass carbon sink of Canada's boreal forests. PNAS 109 (7), 2423–2427. https://doi.org/10.1073/pnas.1111576109.
Man, R., Colombo, S., Lu, P., Li, J., Dang, Q.L., 2014. Trembling aspen, balsam poplar, and white birch respond differently to experimental warming in winter months. Can. J. For. Res. 44 (12), 1469–1476. https://doi.org/10.1139/cjfr-2014-0302.
Melillo, J.M., Butler, S., Johnson, J., Mohan, J., Steudler, P., Lux, H., Tang, J., 2011. Soil warming, carbon-nitrogen interactions, and forest carbon budgets. PNAS 108 (23), 9508–9512. https://doi.org/10.1073/pnas.1018189108.
Michaelian, M., Hogg, E.H., Hall, R.J., Arsenault, E., 2011. Massive mortality of aspen following severe drought along the southern edge of the Canadian boreal forest. Glob. Chang. Biol. 17 (6), 2084–2094. https://doi.org/10.1111/j.1365-2486.2010.02357.x.
Pan, Y., Birdsey, R.A., Fang, J., Houghton, R., Kauppi, P.E., Kurz, W.A., Hayes, D., 2011. A large and persistent carbon sink in the world's forests. Science 333 (6045), 988–993. https://doi.org/10.1126/science.1201609.
Pan, Y., Luo, T., Birdsey, R., Hom, J., Melillo, J., 2004. New estimates of carbon storage and sequestration in China's forests: effects of age–class and method on inventory-based carbon estimation. Clim. Chang. 67 (2), 211–236. https://doi.org/10.1007/s10584-004-2799-5.

Payette, S., Shugart, H.H., Leemans, R., Bonan, G.B., 1992. Fire as a controlling process in the North American boreal forest. A Systems Analysis of the Global Boreal Forest. Cambridge University Press, Cambridge, U.K, pp. 144–169.

Pregitzer, K.S., Euskirchen, E.S., 2004. Carbon cycling and storage in world forests: biome patterns related to forest age. Glob. Chang. Biol. 10 (12), 2052–2077. https://doi.org/10.1111/j.1365-2486.2004.00866.x.

R Development Core Team, 2016. R: A Language and Environment for Statistical Computing. R Foundation for Statistical Computing, Vienna, Austria. https://www.R-project.org.

Ray, R., Ganguly, D., Chowdhury, C., Dey, M., Das, S., Dutta, M.K., Jana, T.K., 2011. Carbon sequestration and annual increase of carbon stock in a mangrove forest. Atmos. Environ. 45 (28), 5016–5024. https://doi.org/10.1016/j.atmosenv.2011.04.074.

RStudio Team, 2016. RStudio: Integrated Development for R. RStudio, Inc., Boston, Massachusetts, USA. http://www.rstudio.com.

SFAPRC, 2011. Technical Regulations for Inventory for Forest Management Planning and Design. https://www.doc88.com/p-9962134492051.html (accessed 13 January 2023).

Shen, H., Zhang, W., Cao, J., Zhang, X., Xu, Q., Yang, X., Zhao, Y., 2016. Carbon concentrations of components of trees in 10-year-old Populus davidiana stands within the desertification combating program of Northern China. Front. Earth Sci. 10 (4), 662–668. https://doi.org/10.1007/s11707-016-0562-7.

Shi, F., Sasa, K., Koike, T., Osawa, A., Zyryanova, O.A., Matsuura, Y., Kajimoto, T., Wein, R.W., 2010. Characteristics of Larch Forests in Daxingan Mountains, Northeast China. Permafrost Ecosystems: Siberian Larch Forests. Ecological Studies. Springer, Dordrecht, pp. 367–383.

Shugart, H., Sedjo, R., Sohngen, B., 2003. Forests & Global Climate Change: Potential Impacts on U.S. Forest Resources. Pew Center on Global Climate Change, Arlington, VA. https://www.sierraforestlegacy.org/Resources/Conservation/FireForestEcology/ThreatsForestHealth/Climate/CI-PewCenterforGlobalClimateChangeForestReport2003.pdf. accessed 13 January 2023.

Shvidenko, A., 2011. Changing world, boreal forests and IBFRA. Keynote speeches. Boreal forests in a changing world: challenges and needs for action. In: Proceedings of the International Conference IBFRA. Krasnoyarsk, Russia. August 15-21 2011. https://core.ac.uk/download/pdf/33901253.pdf. accessed 13 January 2023.

Silva, L.C.R., Anand, M., 2013. Probing for the influence of atmospheric CO_2 and climate change on forest ecosystems across biomes. Glob. Ecol. Biogeogr. 22 (1), 83–92. https://doi.org/10.1111/j.1466-8238.2012.00783.x.

Sohngen, B., Sedjo, R., 2005. Impacts of climate change on forest product markets: implications for North American producers. For. Chronicle 81 (5), 669–674. https://doi.org/10.5558/tfc81669-5.

Soja, A.J., Tchebakova, N.M., French, N.H.F., Flannigan, M.D., Shugart, H.H., Stocks, B. J., Stackhouse, P.W., 2007. Climate-induced boreal forest change: predictions versus current observations. Global Planet. Change 56 (3), 274–296. https://doi.org/10.1016/j.gloplacha.2006.07.028.

Strassburg, B.B.N., Kelly, A., Balmford, A., Davies, R.G., Gibbs, H.K., Lovett, A., Rodrigues, A.S.L., 2010. Global congruence of carbon storage and biodiversity in terrestrial ecosystems. Conserv. Lett. 3 (2), 98–105. https://doi.org/10.1111/j.1755-263X.2009.00092.x.

Tang, X., Zhao, X., Bai, Y., Tang, Z., Wang, W., Zhao, Y., Zhou, G., 2018. Carbon pools in China's terrestrial ecosystems: new estimates based on an intensive field survey. PNAS 115 (16), 4021–4026. https://doi.org/10.1073/pnas.1700291115.

Tao, J., Zhang, Y., Yuan, X., Wang, J., Zhang, X., 2013. Analysis of forest fires in Northeast China from 2003 to 2011. Int. J. Remote Sens. 34 (22), 8235–8251. https://doi.org/10.1080/01431161.2013.837229.

Thomas, S.C., Malczewski, G., 2007. Wood carbon content of tree species in Eastern China: interspecific variability and the importance of the volatile fraction. J. Environ. Manag. 85 (3), 659–662. https://doi.org/10.1016/j.jenvman.2006.04.022.

Tsogtbaatar, J., 2004. Deforestation and reforestation needs in Mongolia. For. Ecol. Manag. 201 (1), 57–63. https://doi.org/10.1016/j.foreco.2004.06.011.

Van Bogaert, R., Jonasson, C., De Dapper, M., Callaghan, T.V., 2009. Competitive interaction between aspen and birch moderated by invertebrate and vertebrate herbivores and climate warming. Plant Ecolog. Divers. 2 (3), 221–232. https://doi.org/10.1080/17550870903487456.

Waelbroeck, C., 1993. Climate-soil processes in the presence of permafrost: a systems modelling approach. Ecol. Model. 69 (3), 185–225. https://doi.org/10.1016/0304-3800(93)90027-P.

Wang, C., Gower, S.T., Wang, Y., Zhao, H., Yan, P., Bond-Lamberty, B.P., 2001. The influence of fire on carbon distribution and net primary production of boreal Larix gmelinii forests in north-eastern China. Glob. Chang. Biol. 7 (6), 719–730. https://doi.org/10.1046/j.1354-1013.2001.00441.x.

Wang, X., Pederson, N., Chen, Z., Lawton, K., Zhu, C., Han, S., 2019. Recent rising temperatures drive younger and southern Korean pine growth decline. Sci. Total Environ. 649, 1105–1116. https://doi.org/10.1016/j.scitotenv.2018.08.393.

Xu, H., 1998. Forests in Daxing'anling Mountains China. Science Press, Beijing, China.

Yu, D., Zhou, L., Zhou, W., Ding, H., Wang, Q., Wang, Y., Dai, L., 2011. Forest management in Northeast China: history, problems, and challenges. Environ. Manag. 48 (6), 1122–1135. https://doi.org/10.1007/s00267-011-9633-4.

Yun, R., Jin, Y., Li, J., Chen, Z., Lyu, Z., Zhao, Y., Cui, D., 2021. The annual rhythmic differentiation of Populus davidiana growth–climate response under a warming climate in The Greater Hinggan Mountains. Glob. Ecol. Conserv. 27, e01549. https://doi.org/10.1016/j.gecco.2021.e01549.

Zhang, Q., Wang, C., Wang, X., Quan, X., 2009. Carbon concentration variability of 10 Chinese temperate tree species. For. Ecol. Manag. 258 (5), 722–727. https://doi.org/10.1016/j.foreco.2009.05.009.

Zhang, X., Liu, X., Zhang, Q., Zeng, X., Xu, G., Wu, G., Wang, W., 2018. Species-specific tree growth and intrinsic water-use efficiency of Dahurian larch (Larix gmelinii) and Mongolian pine (Pinus sylvestris var. mongolica) growing in a boreal permafrost region of the Greater Hinggan Mountains, Northeastern China. Agric. For. Meteorol. 248, 145–155. https://doi.org/10.1016/j.agrformet.2017.09.013.

Zhou, C., Wei, X., Zhou, G., Yan, J., Wang, X., Wang, C., Zhang, Q., 2008. Impacts of a large-scale reforestation program on carbon storage dynamics in Guangdong, China. For. Ecol. Manag. 255 (3), 847–854. https://doi.org/10.1016/j.foreco.2007.09.081.

Zhu, B., Wang, X., Fang, J., Piao, S., Shen, H., Zhao, S., Peng, C., 2010. Altitudinal changes in carbon storage of temperate forests on Mt Changbai, Northeast China. J. Plant Res. 123 (4), 439–452. https://doi.org/10.1007/s10265-009-0301-1.